N-Doped TiO2 Photocatalyst Coatings Synthesized by a Cold Atmospheric Plasma

Article *in* Langmuir · May 2019

DOI: 10.1021/acs.langmuir.9b00784

12 authors, including:

Qianqian Chen
Université Libre de Bruxelles
12 PUBLICATIONS **181** CITATIONS
SEE PROFILE

Alp Ozkan
Université Libre de Bruxelles
15 PUBLICATIONS **162** CITATIONS
SEE PROFILE

Basab Chattopadhyay
Norwegian University of Science and Technology
61 PUBLICATIONS **847** CITATIONS
SEE PROFILE

K. Baert
Vrije Universiteit Brussel
47 PUBLICATIONS **449** CITATIONS
SEE PROFILE

LANGMUIR Article
Cite This: Langmuir 2019, 35, 7161−7168
pubs.acs.org/Langmuir

N-Doped TiO_2 Photocatalyst Coatings Synthesized by a Cold Atmospheric Plasma

Qianqian Chen,*[,†] Alp Ozkan,[†] Basab Chattopadhyay,[‡] Kitty Baert,[§] Claude Poleunis,[∥] Alisson Tromont,[⊥] Rony Snyders,[⊥,#] Arnaud Delcorte,[∥] Herman Terryn,[§] Marie-Paule Delplancke-Ogletree,[▽] Yves H. Geerts,[‡] and François Reniers*[,†]

[†]Chemistry of Surfaces, Interfaces, and Nanomaterials and [‡]Laboratoire de Chimie des Polymères, Faculté des Sciences, Université Libre de Bruxelles, ULB Boulevard du Triomphe, Brussels 1050, Belgium

[§]Research Group Electrochemical and Surface Engineering, Vrije Universiteit Brussel, Pleinlaan 2, 1050 Brussels Belgium

[∥]Institute of Condensed Matter and Nanosciences, Université Catholique de Louvain, 1348 Louvain-la-Neuve, Belgium

[⊥]Materia Nova Research Center, Parc Initialis, B-7000 Mons, Belgium

[#]ChIPS, CIRMAP, Université de Mons, 23 Place du Parc, B-7000 Mons, Belgium

[▽]4MAT, CP 165/63, Université Libre de Bruxelles, 50 Av. F.D. Roosevelt, B-1050 Brussels, Belgium

ABSTRACT: This work presents a simple, fast (20 min treatment), inexpensive, and highly efficient method for synthesizing nitrogen-doped titanium dioxide (N-TiO_2) as an enhanced visible light photocatalyst. In this study, N-TiO_2 coatings were fabricated by atmospheric pressure dielectric barrier discharge (DBD) at room temperature. The composition and the chemical bonds of the TiO_2 and N-TiO_2 coatings were characterized by X-ray photoelectron spectroscopy (XPS) and time-of-flight secondary ion mass spectroscopy (ToF-SIMS). The results indicate that the nitrogen element has doped the TiO_2 lattice, which was further confirmed by Raman spectroscopy and grazing incidence X-ray diffraction (GIXRD). The doping mechanism was investigated using OES to study the plasma properties under different conditions. It suggests that the NH radicals play a key role in doping TiO_2. The concentration of nitrogen in the N-TiO_2 coatings can be controlled by changing the concentration of NH_3 in the plasma or the applied power to adjust the concentration of NH radicals in the plasma. The band gap of N-TiO_2 was reduced after NH_3/Ar plasma treatment from 3.25 to 3.18 eV. Consequently, the N-TiO_2 coating showed enhanced photocatalytic activity under white-light-emitting-diode (LED) irradiation. The photocatalytic degradation rate for the N-TiO_2 coating was about 1.4 times higher than that of the undoped TiO_2 coating.

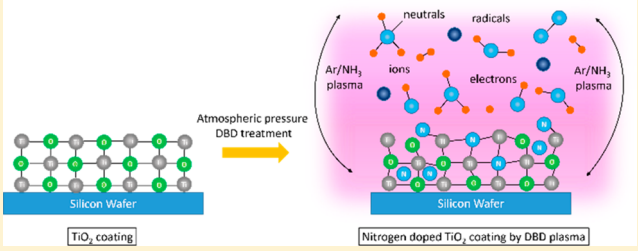

INTRODUCTION

Titanium dioxide (TiO_2) is one of the most promising sustainable photocatalysts for pollutant removal.[1−3] However, the wide band gap (~3.2 eV) of TiO_2 limits its excitation region in the ultraviolet (UV) range (wavelength λ < 388 nm), which constitutes only about 5% of the solar spectrum energy.[2] With the purpose of utilization for the application of TiO_2 in a wider solar spectrum, enhancing the energy absorption to the visible light range is an interesting approach to improving its properties.

In recent years, visible-light-active TiO_2 materials doped with nonmetal impurities were regarded as one of the most promising techniques to reduce the band gap of TiO_2.[3−5] Among several dopants, on the basis of the electronic band structures calculation,[5−7] nitrogen (N) has been identified as a preferred candidate. The formation of a substitution N 2p band above the O 2p valence band narrows the band gap of TiO_2, and the optical absorption of doped TiO_2 shifts to the visible light region.[5,8−10] Besides, compared with other nonmetal elemental doping, N-doped TiO_2 materials show higher enhanced photocatalytic activity and stronger optical absorption with visible light irradiation.[9]

Several methods are used for the preparation of N-doped TiO_2,[9−13] including physical methods and chemical methods. N-TiO_2 thin films were successfully synthesized by high-power impulse magnetron sputtering plasma at a pressure of 0.93 Pa and for a treatment time of 120 min. The authors showed that the energy gap of the TiO_2 film was reduced from 3.45 to 3.40 eV after doping.[11] Yang and co-workers[9] prepared N-doped TiO_2 by the solvothermal method, which showed enhanced absorption in the visible light region and exhibited high photocatalytic activity for the degradation of model dyes. It had been shown that N doping, with Ti^{3+} ions and oxygen vacancies, made contributions to the visible light absorption of

Received: March 16, 2019
Revised: May 8, 2019
Published: May 10, 2019

DOI: 10.1021/acs.langmuir.9b00784
Langmuir 2019, 35, 7161−7168

N-doped TiO_2. Kosowska and co-workers[13] investigated N-doped TiO_2 catalysts by the calcination of hydrated amorphous TiO_2 particles in a gaseous NH_3 atmosphere at 100−800 °C for 4 h. The modified TiO_2 exhibited visible light photocatalytic activity with a reduced band gap of 2.64 eV. Even though the above-mentioned modification methods show that nitrogen has doped TiO_2 successfully, the recognized drawbacks of these methods are that they are time- and energy-consuming.

Plasma-related techniques are environmentally friendly, energy-saving methods that involve high-energy species such as electrons, atoms, and radicals for surface modification and chemistry to impart a variety of physiochemical properties to various materials.[14,15] The dielectric barrier discharge (DBD) plasma, one of the nonthermal plasmas characterized by a high electron temperature (10^4−10^5 °C) but a low bulk gas temperature (as low as room temperature), can be operated at atmospheric pressure, which is a promising technique for catalyst modification. While high temperature and solvent-based treatments are required on the basis of the methods listed above, plasma-assisted doping is conducted at a relatively low temperature without changing the morphology or the structure of TiO_2. Some recent studies have shown a positive effect of plasma treatment on surface modifications.[14−17] Since NH_3 plasma consists of various nitriding species and excited hydrogen,[16,18] NH_3 plasma irradiation on the surface of TiO_2 powders induced an improvement in the photocatalytic properties under visible light.[14] Plasma nitridation of tool steel under atmospheric pressure was performed by $Ar/N_2/H_2$ DBD, resulting in the formation of a uniform nitride layer and a 2-fold surface hardness compared with the original one.[15] Multiwall carbon nanotubes (MWCNTs) were modified using microwave-excited NH_3/Ar plasma.[19] Nitrogen-containing groups were introduced onto the surfaces of the MWCNTs, and the hydrophilicity of the modified MWCNTs was improved.

In the present study, we propose a simple method to synthesize N-doped TiO_2 materials at room temperature involving DBD under atmospheric pressure. This study aims to (i) introduce nitrogen into the TiO_2 lattice by a NH_3/Ar mixture plasma treatment and investigate the evolution of the compositions and the structures; (ii) study the doping mechanisms of TiO_2 by NH_3/Ar plasma with optical emission spectroscopy (OES); and (iii) estimate the photocatalytic performance through the degradation of methylene blue (MB) underexposure of white-light-emitting-diode (LED) lamps.

EXPERIMENTAL SECTION

Preparation of TiO_2 and N-TiO_2 Films. The plasma reactor (shown in Figure 1) is a homemade atmospheric pressure DBD reactor. The DBD reactor chamber is made of glass with a diameter of 210 mm and a wall thickness of 6 mm. Two copper electrodes of 75 mm diameter are inside the chamber, and the plasma is generated in between. Each electrode is covered with a 3-mm-thick alumina barrier, and the electrode gap is 3 mm. An AFS G10S-V AC power supply, operating at 2.7 kHz, is connected to the high-voltage electrode. A half piece of the silicon wafer ((001), 5.08 cm diameter) is used as the substrate, which is cleaned by isopropanol and methanol successively before each deposition. Prior to deposition, the chamber is pumped down to a pressure of 4.5 Torr and then backfilled with Ar to atmospheric pressure to avoid air contamination. TTIP (titanium isopropoxide, 97%, Sigma-Aldrich), heated to 343 K, is used as a precursor for titanium and is introduced directly into the chamber as a vapor carried by an Ar flux. The pipeline between the bubbler and the chamber is heated to 373 K to prevent any condensation of the precursor on it. Moreover, the temperature of the substrate is set at 423 K (measured by an infrared thermometer before and after the deposition). During the deposition processes, the gas flow rate is 2 slm for the carrier gas (Ar) and 0.5 slm for O_2. The applied power is 30 W, and the deposition time is 10 min. According to our earlier studies, the as-deposited TiO_2 films are amorphous.[20] Therefore, a heat treatment (annealing in air) at 723 K for 2 h is used to get the crystalline TiO_2 films. This preparation method has been described in ref 20.

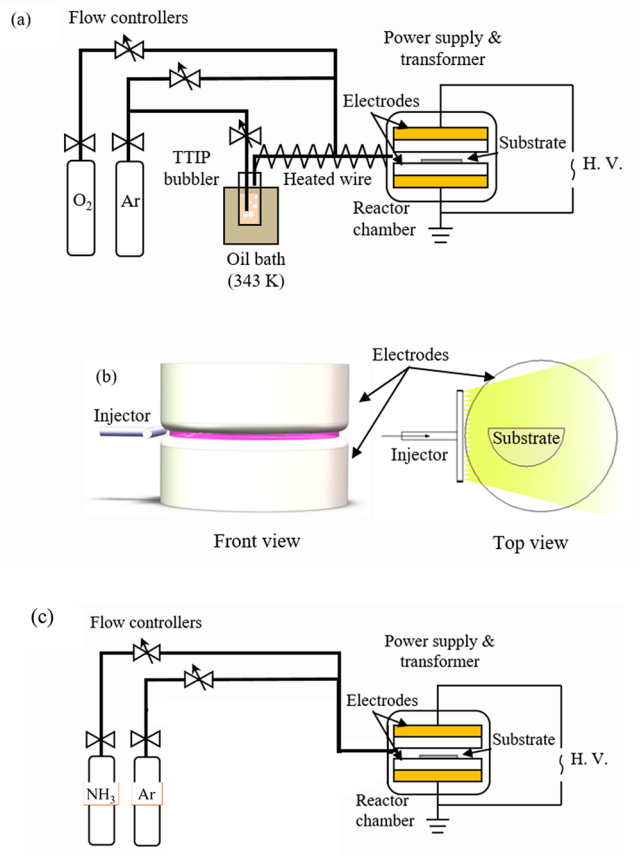

Figure 1. Schematic of (a) the experimental setup for the deposition of TiO_2 films, (b) the detailed designs of the DBD reactor systems, and (c) the experimental setup for doping.

The annealed TiO_2 films are used to prepare N-doped TiO_2 films using the same system that is used for deposition. The annealed TiO_2 films are put onto the middle of the bottom electrode, which is used without any heating, and exposed to an Ar/NH_3 DBD plasma. Prior to any treatment, the chamber is pumped down to remove air and then backfilled with Ar. Afterward, 2 slm of Ar and NH_3 is injected into the chamber. Then, the DBD plasma is lighted up at room temperature. After 20 min of treatment, the resulting coating (denoted as N-TiO_2) is obtained. To study the doping mechanism, different concentrations of NH_3 (the flow rate ratio of NH_3 to Ar varied from 0.5 to 5%) and different applied powers (30−100 W) were used.

Characterization. XPS analysis is performed on the PHI 5600ci spectrometer with an Mg X-ray source (Kα = 1253.6 eV) under vacuum of about 10^{-9} Torr at 200 W operated at 14 kV. Both survey scans (187.85 eV pass energy, with 0.25 eV/step, three sweeps) and high-resolution scans (23.5 eV pass energy, with 0.05 eV/step, five sweeps) are recorded. The spectra are calibrated according to the C 1s peak at 284.6 eV as a reference. The Casa XPS software is used for data interpretation using a Shirley background. The sensitivity coefficients are from the manufacturer's handbook: S_C = 0.205, S_O = 0.63, S_N = 0.38, and S_{Ti} = 1.1.

DOI: 10.1021/acs.langmuir.9b00784
Langmuir 2019, 35, 7161−7168

For XPS analysis, some samples are subjected to Ar^+ sputtering to remove the surface contamination. Ar sputtering is performed using a 4 keV beam rastered over 2 × 2 mm^2.

For the depth profile acquired in this study, time-of-flight secondary ion mass spectra (ToF-SIMS) were recorded using an ion ToF instrument (GmbH, Münster, Germany). Cs^+ (1 keV) with 100 nA current is used to create an area of 500 × 500 μm^2, and the middle 200 × 200 μm^2 is analyzed using a pulsed 0.6 pA Bi^{3+} primary ion beam at a 30 kV accelerating voltage. The positive secondary ion mass spectra are calibrated using C^+, TiO^+, TiN^+, and $TiON^+$. All data analyses are carried out using the software supplied by the instrument manufacturer, SurfaceLab.

The use of grazing incidence X-ray Diffraction (GIXRD, Rigaku Ultima IV diffractometer) was used to determine the crystallinity of the film. The GIXRD spectra are recorded at a constant angle of incidence of 0.5° with Cu Kα (λ = 1.5418 Å) irradiation.

Raman microscopy (LabRAM HR Evolution, HORIBA Scientific) is also used to identify the crystallinity of the films. It is equipped with a multichannel air-cooled CCD detector (spectral resolution <1 cm^{-1}, lateral resolution 0.5 μm, axial resolution 2 μm) and a solid-state laser corresponding to green light (532 nm) and works at 1.25 mW excitation with a 10% filter.

The surface morphology and the film thickness of the deposited films are examined using a scanning electron microscope (SEM, Hitachi SU 70) operating at 20 kV.

Optical emission spectroscopy (OES) diagnostics allow us to determine and evaluate some specific excited species in the plasma phase. It is performed with an Andor Shamrock-500i spectrometer (0.500 m focal length, triple grating imaging) including an Andor DU420A-OE CCD camera.

Photocatalytic Activity Tests. Methylene blue (MB) is utilized as a model dye to evaluate the photocatalytic activity of the films. The degradation of MB is carried out by self-made equipment. White-light-emitting-diode (LED) lamps (10 W, Philip) are used as the visible light source.[21] The distance between the LED lamps and the fluid level is kept at 150 mm. Thirty milliliters of 5 mg L^{-1} aqueous MB is added to a glass Petri dish with a diameter of 60 mm. The as-prepared N-doped TiO_2 film (half of the Si wafer, about 10 cm^2) sinks to the bottom of the Petri dish. Before the photoreaction procedures, the system is stirred by magnetic force in the dark for 30 min to ensure the adsorption equilibrium. During the photodegradation process, about 2 mL of the solution is placed in a cuvette at 30 min intervals, and the absorption spectra of the obtained solutions are obtained by UV−vis spectroscopy (UV-3100 PC, VWR).

RESULTS AND DISCUSSION

The chemical composition of TiO_2 and N-TiO_2 coatings is investigated using XPS survey spectra and high-resolution Ti 2p and N 1s spectra (Figure 2). After removing the surface contamination by sputtering, for both samples, the survey spectra (Figure 2a) show the presence of O, Ti, and a small amount of C. However, there is a small N 1s peak in the N-TiO_2 coating, with a 2.64% concentration.

Since sputtering modifies the shape of Ti 2p peaks by reducing Ti^{4+} to Ti^{3+} on the surface, the high-resolution spectra of Ti 2p shown were acquired before sputtering. In Figure 2b, the XPS spectrum of the Ti 2P core level obtained from the TiO_2 coating exhibited a Ti $2p_{3/2}$ peak at 458.6 eV and Ti $2p_{1/2}$ at 464.3 eV. After treatment in the Ar/NH_3 discharge, the binding energies of Ti $2p_{3/2}$ and Ti $2p_{1/2}$ of the N-TiO_2 shift to 458.4 and 464.1 eV, respectively. This small shift could be attributed to the electronic interactions of Ti with nitrogen. It is known that the electronegativity of nitrogen is lower than that of oxygen.[1,2,8,14] On the other hand, it has been reported that the incorporation of N atoms into the TiO_2 lattice can also lead to the shift of the Ti 2p peaks to lower binding energies.[8] However, because of the small value of the observed shift (0.2−0.3 eV), which is in the range of the error of the spectrometer, it cannot be accepted as absolute proof of N-doping.

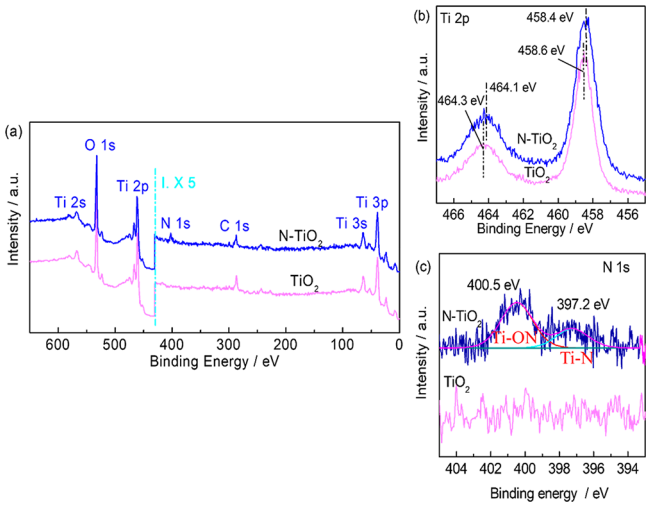

Figure 2. (a) After sputtering XPS survey spectra and high-resolution spectra of (b) Ti 2p (before sputtering) and (c) N 1s (after sputtering) for TiO_2 and N-TiO_2 coatings treated under 1% NH_3 and 100 W.

One of the most interesting results is shown in the N 1s XPS spectra depicted in Figure 2c. It shows a complex signal of nitrogen at 400.5 and 397.2 eV only in N-TiO_2, which is consistent with the presence of a small N peak in the survey spectra. According to some other recent studies under the same type of conditions,[11,12,22,23] the binding energy at 400.5 eV could be assigned to a Ti−O−N structure, characteristic of interstitial N atoms. A variety of peaks with N 1s binding energies comprised between 395.8 and 397.8 eV were already found in other works,[11,23−25] which are widely regarded as substitutional nitrogen. The variations in the binding energy within this range can be explained by a variation in the oxygen to nitrogen ratio.[25,26] These findings suggest that by the simple atmospheric DBD treatment, N may be introduced into TiO_2 lattices both as the interstitial and substitutional dopants. Similar results on the N 1s chemical states of N-doped TiO_2 have also been achieved by using an NH_x^+ ion implantation method in a UHV (ultrahigh vacuum) chamber at room temperature or at 527 °C.[23]

To further prove that nitrogen is present in the TiO_2 lattice and does not just cover the surface, TOF-SIMS depth profiles of the films are performed and presented in Figure 3. The intensity of different positive ion species is plotted against the Cs^+ sputter fluence for the N-TiO_2 film. A signal attributed to

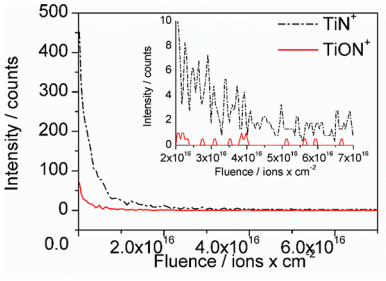

Figure 3. SIMS depth profiling of N-TiO_2 coating treated under 1% NH_3 and 100 W.

DOI: 10.1021/acs.langmuir.9b00784
Langmuir 2019, 35, 7161−7168

Ti-ON$^+$ and TiN$^+$ is observed in the depth profiles, which decreases with higher sputter fluence. These results confirm (i) nitrogen incorporation into these films in Ti−O−N and Ti−N states and (ii) most of the N is on the surface, especially in the state of Ti−N, while a small amount of Ti−N is distributed through the coating.

However, uncertainty remains for the interstitial or substitutional nature of the doping. The high-resolution N 1s scan (Figure 2c) shows that most of the nitrogen is interstitial (Ti−O−N species) rather than substitutional (N−Ti) from SIMS results (Figure 3), which is also confusing for us. To our understanding, XPS is more for surface characterization, even after a short sputtering time (in our case 48 s), while SIMS is a depth profiling technique.

Further structural analysis of TiO_2 and N-TiO_2 coatings is carried out using XRD, as presented in Figure 4a. With and

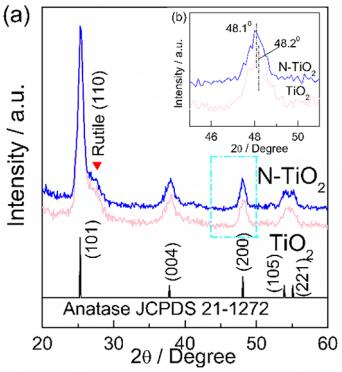

Figure 4. XRD patterns of TiO_2 and N-TiO_2 coatings treated under 1% NH_3 and 100 W.

without the N dopant, both films are crystallized in the anatase phase (JCPDS 21-1272) and present a small amount of rutile. It is widely agreed that the biphase structure is preferred to the single phase for charge separation, leading to a higher photocatalytic efficiency.[27] The results suggest that the phase of the TiO_2 coatings does not change with the addition of nitrogen. The inset in Figure 4b shows the (200) peak position of TiO_2 and N-TiO_2 coatings. A marginal shift of the (200) peak to a smaller degree (higher *d* value) can be noted by the nitrogen incorporation into the TiO_2 crystal lattice. According to refs 26 and 28, a higher *d* value implies compressive residual stress, which may emanate from the differences in the bonding characteristics between nitrogen and oxygen. It might be caused by the N doping when the oxygen is replaced by the nitrogen, resulting in the modification of the electronic states. As a comparison, atmospheric pressure Ar/N_2/H_2 DBD was used to nitride the surface of tool steel by Miyamoto and co-workers.[15] Through the hardness measurement, they showed that the formation of a uniform nitride layer on the steel caused the surface hardness to increase more than 2-fold. It was demonstrated that the shift of the XRD pattern was due to the nitrogen atom solute in the surface of the tool steel.

The phase compositions of TiO_2 and N-TiO_2 coatings are further examined by Raman spectra analysis (Figure 5a).

On the basis of the previously reported literature,[27] six fundamental transitions are expected in the Raman spectrum of the anatase phase of TiO_2 (i.e., 144 cm^{-1} (E_g), 197 cm^{-1} (E_g), 399 cm^{-1} (B_{1g}), 513 cm^{-1} (A_{1g}), 519 cm^{-1} (B_{1g}), and 639 cm^{-1} (E_g)). Four Raman bands at 143 cm^{-1} (B_{1g}), 447 cm^{-1}

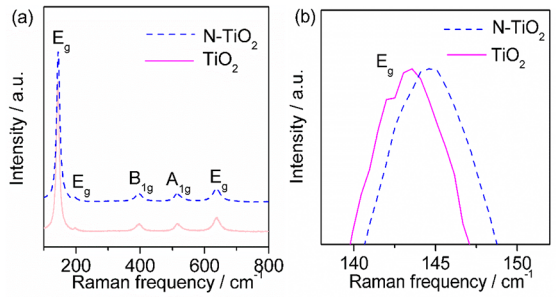

Figure 5. Raman spectra of TiO_2 and N-TiO_2 coating treated under 1% NH_3 and 100 W.

(E_g), 612 cm^{-1} (A_{1g}), and 826 cm^{-1} (B_{2g}) are attributed to the rutile phase. Both the TiO_2 and the N-TiO_2 coatings present the Raman spectra of the anatase phase, with no peaks referring to the rutile phase. However, a small peak is assigned to rutile in the XRD pattern. The absence of the rutile peak in the Raman spectra can be due to the low sensibility of the Raman equipment. Figure 5b shows the enlarged localized profiles of the E_g (144 cm^{-1}) peak of the two coatings. The E_g (144 cm^{-1}) peak slightly shifts toward higher wavenumbers from TiO_2 to N-TiO_2. On the basis of the existing literature, the shift effect is indicative of lattice disorder defects. It can be caused by oxygen vacancies,[29,30] the electronic interaction between titania and nitrogen doping,[27,31] or the change in particle size.[32,33]

SEM is also employed to characterize the microstructure of the films and to provide more evidence about the shift in Raman spectra. The cross-sectional images of the TiO_2 film and N-TiO_2 film are shown in Figure 6. Here, it is noteworthy

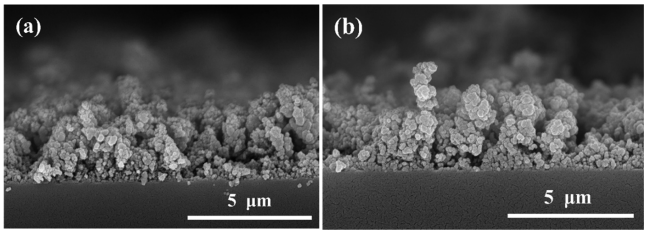

Figure 6. Cross-sectional SEM images of (a) TiO_2 and (b) N-TiO_2 coatings treated under 1% NH_3 and 100 W.

that for TiO_2 and N-TiO_2 films the mean particle sizes are 114 ± 2 and 116 ± 3 nm, respectively. The average mass loading of the films is about 0.36 mg/cm^2. This result also excludes the hypothesis that the particle size is responsible for the shift in the Raman spectra.

To evaluate the modification mechanism with the NH_3/Ar mixture plasma, OES is used to diagnose reactive species and uncover the plasma chemical processes in DBD. Two main wavelength ranges are presented in Figure 7: 300−400 nm (Figure 7a) to study the NH emission spectra and 650−900 nm (Figure 7b) to observe the Ar I emission lines. The peak at 336.0 nm is identified as the NH ($c^1\Pi(v' = 0)$) → $X^3\Sigma(v'' = 1)$ radical, while the peak at 337.1 nm is identified as the NH ($A^3\Pi(v' = 1)$) → $X^3\Sigma(v'' = 1)$ as well as the second positive system (SPS $C^3\Pi_u$→ $B^3\Pi_g$) of N_2.[16,34] Compared to the spectra of the pure argon plasma, NH radicals at 336.0 nm obviously appear in the spectra of the Ar/NH_3 plasma (shown in Figure 7a). The peak of N_2 at 337.1 nm appears in both spectra and originates from air contamination. In NH_3/Ar

DOI: 10.1021/acs.langmuir.9b00784
Langmuir 2019, 35, 7161−7168

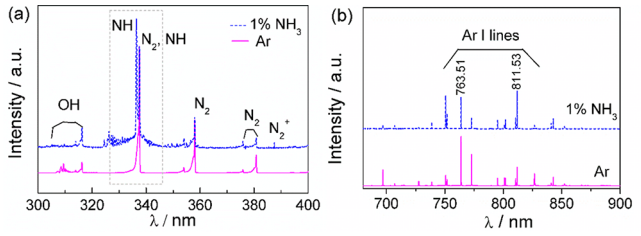

Figure 7. Optical emission spectra of plasma with 1% and without NH_3 under 100 W in the (a) 300–400 and (b) 650–900 nm ranges.

plasma shown in Figure 7b, the intensity of Ar I at 763.51 and 811.53 nm indexed to $2p_6 \rightarrow 1s_5$, $2p_9 \rightarrow 1s_5$ (Paschen notation of the terms) transitions, respectively, which contributed to the Ar metastable states, decreases compared to pure Ar plasma. In addition, other fraction productions such as for N_2^+ radicals, which show a peak at 387.6 nm, possibly also partially contribute to the introduction of the nitrogen group in the coating.

The analysis assumes that the NH radicals are generated by electron-driven collisional excitation, ionization reactions, and Penning ionization with a subsequent quenching effect. Chemical reactions between argon metastable atoms and ammonia molecules, including the collisional excitation and ionization reactions, Penning reactions, and quenching, are detailed below.[16,34,35]

Collisional excitation and ionization reactions:

$$e^- + NH_3 \rightarrow NH_3^* + e^- \quad (1)$$

$$e^- + NH_3 \rightarrow NH + 2H + e^- \quad (2)$$

$$e^- + NH_3^* \rightarrow NH + 2H + e^- \quad (3)$$

$$e^- + NH_3 \rightarrow NH_3^+ + 2e^- \quad (4)$$

$$e^- + NH_3^* \rightarrow NH_3^+ + 2e^- \quad (5)$$

Penning reactions:

$$Ar(^3P_2, ^3P_0) + NH_3 \rightarrow NH_3^+ + Ar + e^- \quad (6)$$

$$\rightarrow NH_2 + Ar + H \quad (7)$$

$$\rightarrow NH + Ar + H + H \quad (8)$$

Three-body and binary reactions:

$$NH_2 + H + Ar \rightarrow Ar + NH_3 \quad (9)$$

$$NH_2 + NH_2 + Ar \rightarrow Ar + N_2H_4 \quad (10)$$

$$NH + H + H + Ar \rightarrow Ar + NH_3 \quad (11)$$

$$H + H + Ar \rightarrow Ar + H_2 \quad (12)$$

$$NH + NH \rightarrow 2H + N_2 \quad (13)$$

$$NH + H \rightarrow N + H_2 \quad (14)$$

$$NH_2 + N \rightarrow 2H + N_2 \quad (15)$$

On top of the three-body and binary reactions listed above, direct quenching of NH by NH_3 is also presented, as already reported by Gelernt and Filseth.[36]

The introduction of N into TiO_2 coatings may be related to the concentration of NH radicals in the plasma. For further analysis, the effect of the concentration of NH_3 and the applied power are investigated and presented in Figure 8. It is shown in Figure 8a that an increase in NH_3 concentration at a fixed

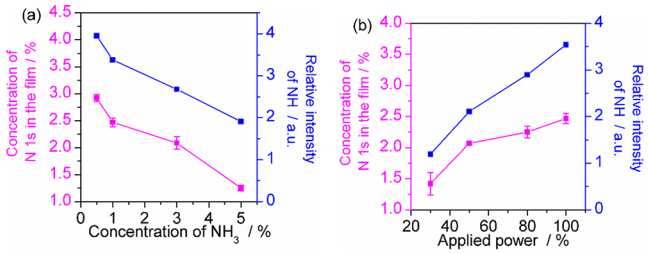

Figure 8. Intensity of the OES NH radical line (336.0 nm) and concentration of N 1s in the TiO_2 films as a function of (a) different concentrations of NH_3, while the flow rate of Ar is 2 slm and the applied power is 100 W, and (b) different applied power, while the concentration of NH_3 is 1% and the flow rate of Ar is 2 slm.

power (100 W) leads to a decrease in the NH content. A similar trend was reported by Fateev and co-workers[16] and Chang and co-workers.[34] Fateev and co-workers explained this effect by the electronegativity of NH_3. Electron capture by ammonia molecules leads to the formation of H^- and NH_2^- negative ions[16] that reduced the formation of NH. Chang and co-workers[34] interpreted this phenomenon with the Penning effect and the quenching effect of NH_3. The Penning effect between metastable Ar and the NH_3 molecule dominates the discharge property. However, the quenching effect of the surplus NH_3 mainly influences the discharge when the concentration of NH_3 is high.[34] An increase in applied power leads to more efficient ammonia decomposition,[16] which causes an increase in the NH signal as shown in Figure 8b. One can notice that the concentration of N in the TiO_2 coatings (based on the XPS results after sputtering) decreases as the relative intensity of NH decreases (based on the OES results). This suggests that the NH radical concentration in the plasma contributes to the doping of the TiO_2 coatings. It was reported that the NH radical may have a higher probability to form a covalent bond or to induce defects on MWCNTs.[19] Truscott and co-workers[37] also reported that NH radicals played a crucial role in the deposition of nitrogen-doped diamond by microwave plasma-activated CVD. Recently, Ciolan and co-workers[38] investigated Ar/NH_3 gas mixture plasma processing onto the RF magnetron-sputtered defective ZnO thin films. They claimed that the concentration of NH in the plasma was maximum at a small amount of NH_3 gas, which is determined from the product of NH_3 concentration and electron density. Similar results were obtained by Oever and co-workers.[39]

To determine the effect of nitrogen-doped TiO_2 on the UV–vis light response, we further studied the optical property of the coatings with UV–vis spectroscopy. The UV–vis DRS spectra of the TiO_2 coatings are shown in Figure 9. The comparison of the spectrum of the TiO_2 coating and the spectrum of the N-TiO_2 coating reveals a red shift of the absorption edge toward the visible region for N-TiO_2 coating (Figure 9a), as was reported by previous works.[1,2,14,40,41] This is attributed to the presence of nitrogen atoms in the TiO_2 lattices, leading to the appearance of N 2p interband energy levels in the TiO_2 band gap just above the upper edge of the valence band.

DOI: 10.1021/acs.langmuir.9b00784
Langmuir 2019, 35, 7161–7168

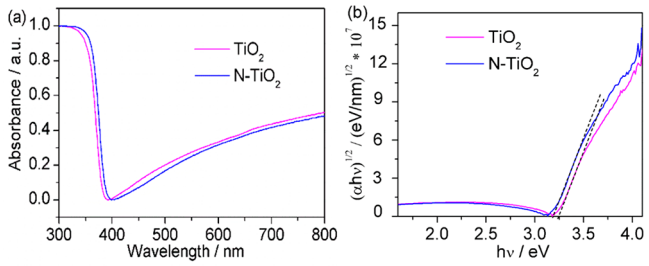

Figure 9. UV−vis diffuse reflectance spectra (DRS) of undoped (purple curve) and N-doped (blue curve) TiO_2 coatings treated under 1% NH_3 and 100 W (a) and the corresponding $(\alpha h\nu)^{1/2}$ versus $h\nu$ plots used to determine the optical band gaps (b).

The band gaps of TiO_2 and N-TiO_2 are estimated by using Tauc plots,[2,42] as shown in Figure 9b. To do this, $(\alpha h\nu)^{1/2}$ vs $h\nu$ is plotted according to the equation

$$(\alpha h\nu)^{1/2} = k(h\nu - E_g)$$

where α is the absorption coefficient, $h\nu$ is the photon energy, k is a constant, and E_g is the band gap. The absorption coefficient is estimated from the equation

$$\alpha = \frac{1}{d}\ln\left[\frac{1-R^2}{T(\lambda)}\right]$$

where d is the thickness, R is the reflectance, and $T(\lambda)$ is the transmittance of the film. The linear portion of the Tauc plot intersects the X axis at $(\alpha h\nu)^{1/2} = 0$. The values of E_g have been estimated from this intercept.[43,44] As calculated, the band gap of the N-TiO_2 coating is 3.18 eV and that of the undoped TiO_2 coatings is 3.25 eV. This supports the proof that the NH_3/Ar plasma treatment reduces the band gap of TiO_2.

The photocatalysis of TiO_2 and N-TiO_2 coatings has been carried out by degrading MB under white LED light irradiation. Figure 10a illustrates the degradation of MB as a

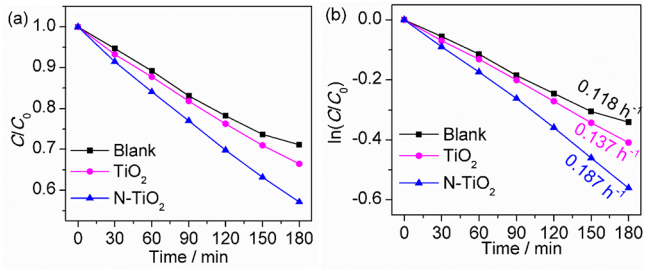

Figure 10. Relative concentration curves of MB aqueous solutions (initial concentration: 5 mM) under different experimental conditions under white LED irradiation (a) and first-order kinetics (b).

function of irradiation time in the presence of TiO_2 and N-TiO_2 films and the control experiment. It shows that in the absence of the catalysts MB is subjected to photolysis, resulting in the decrease in the absorbance after 180 min of irradiation. The MB degradation with the TiO_2 coating reaches 34% after 180 min of irradiation. Compared to the TiO_2 coating, the catalytic efficiency of N-TiO_2 is evidently enhanced by 43% degradation under the same conditions. The linear relationship of $\ln(C/C_0)$ versus time (Figure 10b) suggests that the photocatalytic degradation of the MB solution follows pseudo-first-order kinetics. The photocatalytic degradation rate constant for the N-TiO_2 coating is 0.187 h^{-1}, about 1.4 times higher than that of the undoped TiO_2 coating (0.137 h^{-1}). This result further confirms a successful plasma treatment for the enhancement of the N-TiO_2 coatings' photocatalytic activity.

CONCLUSIONS

This study reports the simple, fast, and efficient nitrogen doping of a TiO_2 coating using a room-temperature NH_3/Ar DBD operating at atmospheric pressure. XPS and SIMS results indicate the nitrogen doping of the TiO_2 lattice. Uncertainty remains for the interstitial or substitutional nature of the doping, as XPS suggests TiON and SIMS TiN. Binding energy shifts in XPS (for Ti 2p), wavenumber shifts in Raman, and the diffraction angle in XRD all suggest nitrogen incorporation into the TiO_2 matrix. All of these shifts are in the error range of the respective technique, and they can therefore not be taken as solid and robust evidence for doping. However, XPS data show that nitrogen is effectively incorporated into the TiO_2 matrix, up to a few percent. This is confirmed by SIMS depth profiling and a change in photocatalytic activity. Both techniques also reveal the presence (in variable amounts) of TiON and TiN components, reinforcing the evidence for doping. The doping mechanism is investigated by OES to study the plasma properties under different conditions. It suggests that the NH radicals play a key role in the TiO_2 doping. The concentration of nitrogen in the N-TiO_2 coatings can be adapted by changing the concentration of NH_3 in the plasma or the applied power. The band gap of N-TiO_2 is significantly reduced after the NH_3/Ar plasma treatment from 3.25 to 3.18 eV. The N-TiO_2 coating shows highly enhanced photocatalytic activity under white LED irradiation. Indeed, the photocatalytic degradation rate constant for the N-TiO_2 coating is improved more than 1.4 times compared to that of the undoped TiO_2 coating.

AUTHOR INFORMATION

Corresponding Authors

*E-mail: Qianqian.Chen@ulb.ac.be. Fax: + 32-2-650-2934. Tel: + 32-2-650-2943.

*E-mail: freniers@ulb.ac.be. Fax: + 32-2-650-2934. Tel: +32-2-650-3116.

ORCID

Qianqian Chen: 0000-0001-9042-3098

Basab Chattopadhyay: 0000-0001-5106-1880

Herman Terryn: 0000-0003-2639-5496

Yves H. Geerts: 0000-0002-2660-5767

François Reniers: 0000-0001-9331-6060

Notes

The authors declare no competing financial interest.

ACKNOWLEDGMENTS

The authors thank the China Scholarship Council (CSC, grant no. 201407040053) for a Ph.D. scholarship (Q.C.) and the Belgian Federal Office for Science Policy (BELSPO) for its financial support through the IAP-VII/12, P7/34 (Interuniversity Attraction Pole) program "PSI-Physical Chemistry of Plasma Surface Interactions". FNRS/FWO EoS (Excellence of Science) project NITROPLASM also contributed to funding this research. B.C. kindly acknowledges financial support from the FRS-FNRS (Belgian National Scientific Research Fund) for POLYGRAD Project 22333186. B.C. is an FRS-FNRS Research Fellow.

DOI: 10.1021/acs.langmuir.9b00784
Langmuir 2019, 35, 7161−7168

REFERENCES

(1) Fujishima, A.; Honda, K. Electrochemical Photolysis of Water at a Semiconductor Electrode. *Nature* **1972**, *238*, 37−38.

(2) Islam, S. Z.; Reed, A.; Wanninayake, N.; Kim, D. Y.; Rankin, S. E. Remarkable Enhancement of Photocatalytic Water Oxidation in N_2/Ar Plasma Treated, Mesoporous TiO_2 Films. *J. Phys. Chem. C* **2016**, *120*, 14069−14081.

(3) Patil, M. K.; Shaikh, S.; Ganesh, I. Recent Advances on TiO_2 Thin Film Based Photocatalytic Applications (A Review). *Curr. Nanosci.* **2015**, *11*, 271−285.

(4) Roose, B.; Pathak, S.; Steiner, U. Doping of TiO_2 for Sensitized Solar Cells. *Chem. Soc. Rev.* **2015**, *44*, 8326−8349.

(5) Asahi, R.; Morikawa, T.; Ohwaki, T.; Aoki, K.; Taga, Y. Visible-light Photocatalysis in Nitrogen-Doped Titanium Oxides. *Science* **2001**, *293*, 269−271.

(6) Sathish, M.; Viswanathan, B.; Viswanath, R. P.; Gopinath, C. S. Synthesis, Characterization, Electronic Structure, and Photocatalytic Activity of Nitrogen-Doped TiO_2 Nanocatalyst. *Chem. Mater.* **2005**, *17*, 6349−6353.

(7) Ansari, S. A.; Khan, M. M.; Ansari, M. O.; Cho, M. H. Nitrogen-doped Titanium Dioxide (N-doped TiO_2) for Visible Light Photocatalysis. *New J. Chem.* **2016**, *40*, 3000−3009.

(8) Wang, J.; Tafen, D. N.; Lewis, J. P.; Hong, Z.; Manivannan, A.; Zhi, M.; Li, M.; Wu, N. Origin of Photocatalytic Activity of Nitrogen-Doped TiO_2 Nanobelts. *J. Am. Chem. Soc.* **2009**, *131*, 12290−12297.

(9) Yang, G.; Jiang, Z.; Shi, H.; Xiao, T.; Yan, Z. Preparation of Highly Visible-Light Active N-Doped TiO_2 Photocatalyst. *J. Mater. Chem.* **2010**, *20*, 5301−5309.

(10) Romero-Gomez, P.; Hamad, S.; Gonzalez, J. C.; Barranco, A.; Espinos, J. P.; Cotrino, J.; Gonzalez-Elipe, A. R. Band Gap Narrowing versus Formation of Electronic States in the Gap in N-TiO_2 Thin Films. *J. Phys. Chem. C* **2010**, *114*, 22546−22557.

(11) Stegemann, C.; Moraes, R. S.; Duarte, D. A.; Massi, M. Thermal Annealing Effect on Nitrogen-Doped TiO_2 Thin Films Grown by High Power Impulse Magnetron Sputtering Plasma Power Source. *Thin Solid Films* **2017**, *625*, 49−55.

(12) Sahoo, M.; Mathews, T.; Antony, R. P.; Krishna, D. N.; Dash, S.; Tyagi, A. K. Physicochemical Processes and Kinetics of Sunlight-Induced Hydrophobic-Superhydrophilic Switching of Transparent N-Doped TiO_2 Thin Films. *ACS Appl. Mater. Interfaces* **2013**, *5*, 3967−3974.

(13) Kosowska, B.; Mozia, S.; Morawski, A. W.; Grzmil, B.; Janus, M.; Kaucki, K. The Preparation of TiO_2-Nitrogen Doped by Calcination of $TiO_2 \bullet xH_2O$ under Ammonia Atmosphere for Visible Light Photocatalysis. *Sol. Energy Mater. Sol. Cells* **2005**, *88*, 269−280.

(14) Li, B.; Zhao, Z.; Zhou, Q.; Meng, B.; Meng, X.; Qiu, J. Highly Efficient Low-Temperature Plasma-Assisted Modification of TiO_2 Nanosheets with Exposed {001} Facets for Enhanced Visible-Light Photocatalytic Activity. *Chem. - Eur. J.* **2014**, *20*, 14763−14770.

(15) Miyamoto, J.; Inoue, T.; Tokuno, K.; Tsutamori, H.; Abraha, P. Surface Modification of Tool Steel by Atmospheric-Pressure Plasma Nitriding Using Dielectric Barrier Discharge. *Tribology online.* **2016**, *11*, 460−465.

(16) Fateev, A.; Leipold, F.; Kusano, Y.; Stenum, B.; Tsakadze, E.; Bindslev, H. Plasma Chemistry in an Atmospheric Pressure Ar/NH_3 Dielectric Barrier Discharge. *Plasma Processes Polym.* **2005**, *2*, 193−200.

(17) Kyzioł, K.; Koper, K.; Kaczmarek, Ł.; Grzesik, Z. Plasmochemical Modification of Aluminum-Zinc Alloys Using NH_3-Ar Atmosphere with Anti-Wear Coatings Deposition. *Mater. Chem. Phys.* **2017**, *189*, 198−206.

(18) Pulsipher, D. J. V.; Fisher, E. R. NH_2 and NH Surface Production in Pulsed NH_3 Plasmas on TiO_2: A Steady-State Probe of Short Pulse Plasmas. *Plasma Processes Polym.* **2013**, *10*, 6−18.

(19) Chen, C.; Liang, B.; Lu, D.; Ogino, A.; Wang, X.; Nagatsu, M. Amino Group Introduction onto Multiwall Carbon Nanotubes by NH_3/Ar Plasma Treatment. *Carbon* **2010**, *48*, 939−948.

(20) Chen, Q.; Liu, Q.; Ozkan, A.; Chattopadhyay, B.; Wallaert, G.; Baert, K.; Terryn, H.; Delplancke-Ogletree, M.-P.; Geerts, Y. H.; Reniers, F. Atmospheric Pressure Dielectric Barrier Discharge Synthesis of Morphology-Controllable TiO_2 Films with Enhanced Photocatalytic Activity. *Thin Solid Films* **2018**, *664*, 90−99.

(21) Wu, D.; Wang, W.; Ng, T. W.; Huang, G.; Xia, D.; Yip, H. Y.; Lee, H. K.; Li, G.; An, T.; Wong, P. K. Visible-Light-Driven Photocatalytic Bacterial Inactivation and Mechanism of Zinc Oxysulfide under LED Light Irradiation. *J. Mater. Chem. A* **2016**, *4*, 1052−1059.

(22) Georgieva, J.; Valova, E.; Armyanov, S.; Tatchev, D.; Sotiropoulos, S.; Avramova, I.; Dimitrova, N.; Hubin, A.; Steenhaut, O. A Simple Preparation Method and Characterization of B and N Co-Doped TiO_2 Nanotube Arrays with Enhanced Photoelectrochemical Performance. *Appl. Surf. Sci.* **2017**, *413*, 284−291.

(23) Kim, Y. K.; Park, S.; Kim, K.; Kim, B. Photoemission Study of N-Doped TiO_2 (110) with NH_3. *J. Phys. Chem. C* **2011**, *115*, 18618−18624.

(24) Palgrave, R. G.; Payne, D. J.; Egdell, R. G. Nitrogen Diffusion in Doped TiO_2 (110) Single Crystals: A Combined XPSand SIMS Study. *J. Mater. Chem.* **2009**, *19*, 8418−8425.

(25) Glaser, A.; Surnev, S.; Netzer, F. P.; Fateh, N.; Fontalvo, G. A.; Mitterer, C. Oxidation of Vanadium Nitride and Titanium Nitride Coatings. *Surf. Sci.* **2007**, *601*, 1153−1159.

(26) Yang, X.; Cao, C.; Erickson, L.; Hohn, K.; Maghirang, R.; Klabunde, K. Photo-catalytic Degradation of Rhodamine B on C-, S-, N-, and Fe-doped TiO_2 under Visible-Light Irradiation. *Appl. Catal., B* **2009**, *91*, 657−662.

(27) Preethi, L. K.; Antony, R. P.; Mathews, T.; Walczak, L.; Gopinath, C. S. A Study on Doped Heterojunctions in TiO_2 Nanotubes: An Efficient Photocatalyst for Solar Water Splitting. *Sci. Rep.* **2017**, *7*, 14314.

(28) Jagadale, T. C.; Takale, S. P.; Sonawane, R. S.; Joshi, H. M.; Patil, S. I.; Kale, B. B.; Ogale, S. B. N-Doped TiO_2 Nanoparticle Based Visible Light Photocatalyst by Modified Peroxide Sol-Gel Method. *J. Phys. Chem. C* **2008**, *112*, 14595−14602.

(29) Naldoni, A.; Allieta, M.; Santangelo, S.; Marelli, M.; Fabbri, F.; Cappelli, S.; Bianchi, C. L.; Psaro, R.; Santo, V. D. Effect of Nature and Location of Defects on Bandgap Narrowing in Black TiO_2 Nanoparticles. *J. Am. Chem. Soc.* **2012**, *134*, 7600−7603.

(30) Kim, C.; Kim, K.-S.; Kim, H. Y.; Han, Y. S. Modification of a TiO_2 Photoanode by Using Cr-Doped TiO_2 with an Influence on the Photovoltaic Efficiency of a Dye-Sensitized Solar Cell. *J. Mater. Chem.* **2008**, *18*, 5809−5814.

(31) Melvin, A. A.; Illath, K.; Das, T.; Raja, T.; Bhattacharyya, S.; Gopinath, C. S. M-Au/TiO_2 (M = Ag, Pd, and Pt) Nano Photocatalyst for Overall Solar Water Splitting: Role of Interfaces. *Nanoscale* **2015**, *7*, 13477−13488.

(32) Choi, H. C.; Jung, Y. M.; Kim, S. B. Size Effects in the Raman Spectra of TiO_2 Nanoparticles. *Vib. Spectrosc.* **2005**, *37*, 33−38.

(33) Zhang, W. F.; He, Y. L.; Zhang, M. S.; Yin, Z.; Chen, Q. Raman Scattering Study on Anatase TiO_2 Nanocrystals. *J. Phys. D: Appl. Phys.* **2000**, *33*, 912−916.

(34) Chang, Z.; Yao, C.; Chen, S.; Zhang, G. Electrical and Optical Properties of Ar/NH_3 Atmospheric Pressure Plasma Jet. *Phys. Plasmas* **2016**, *23*, 093503.

(35) Sarani, A.; Nikiforov, A.; Leys, C. Atmospheric Pressure Plasma Jet in Ar and Ar/H_2O Mixtures: Optical Emission Spectroscopy and Temperature Measurements. *Phys. Plasmas* **2010**, *17*, 063504.

(36) Gelernt, B.; Filseth, S. V.; Carrington, T. Quenching and Radiative Lifetimes for NH(b1Σ+, v'=0). *Chem. Phys. Lett.* **1975**, *36* (2), 238−241.

(37) Truscott, B. S.; Kelly, M. W.; Potter, K. J.; Johnson, M.; Ashfold, M. N. R.; Mankelevich, Y. A. Microwave Plasma-Activated Chemical Vapor Deposition of Nitrogen-Doped Diamond. I. N_2/H_2 and NH_3/H_2 Plasmas. *J. Phys. Chem. A* **2015**, *119*, 12962−12976.

(38) Ciolan, M. A.; Motrescu, I.; Sugiura, K.; Luca, D.; Nagatsu, M. Tailoring the Surface Functionalities of Radio Frequency Magnetron-Sputtered ZnO Thin Films by Ar/NH_3 Gas Mixture Surface-Wave Plasmas. *Langmuir* **2018**, *34* (38), 11253−11263.

DOI: 10.1021/acs.langmuir.9b00784
Langmuir 2019, 35, 7161−7168

(39) Van den Oever, P. J.; Van Helden, J. H.; Lamers, C. C. H.; Engeln, R.; Schram, D. C.; Van de Sanden, M. C. M.; Kessels, W. M. M. Density and Production of NH and NH_2 in an Ar-NH_3 Expanding Plasma Jet. *J. Appl. Phys.* **2005**, *98*, 093301−093310.
(40) Irie, H.; Watanabe, Y.; Hashimoto, K. Nitrogen-Concentration Dependence on Photocatalytic Activity of $TiO_{2-x}N_x$ Powders. *J. Phys. Chem. B* **2003**, *107*, 5483−5486.
(41) Buha, J. Optical Properties and Structure of the TiN-Nitrogen-Doped TiO_2 Nanocomposite. *Appl. Surf. Sci.* **2014**, *321*, 457−463.
(42) Valencia, S.; Marín, J. M.; Restrepo, G. Study of the Bandgap of Synthesized Titanium Dioxide Nanoparticules Using the Sol-Gel Method and a Hydrothermal Treatment. *Open Mater. Sci. J.* **2010**, *4*, 9−14.
(43) Grigorov, K. G.; Oliveira, I. C.; Maciel, H. S.; Massi, M.; Oliveira, M. S.; Amorim, J.; Cunha, C. A. Optical and Morphological Properties of N-doped TiO_2Thin Films. *Surf. Sci.* **2011**, *605*, 775−782.
(44) Hassanien, A. S.; Akl, A. A. Influence of Composition on Optical and Dispersion Parameters of Thermally Evaporated Non-Crystalline $Cd_{50}S_{50-x}Se_x$Thin Films. *J. Alloys Compd.* **2015**, *648*, 280−290.

DOI: 10.1021/acs.langmuir.9b00784
Langmuir 2019, 35, 7161−7168